Progress In Electromagnetics Research M, Vol. 86, 173–182, 2019

Deminiaturized Mode Control Rectangular Dielectric Resonator Antenna

Richa Gupta[1] and Arti Vaish[2, *]

Abstract—A modified feed line wideband circularly Polarized Dielectric Resonator Antenna (CPDRA) operating at 24 GHz is proposed in this paper. Deminiaturization of design is achieved by operating antenna at higher order mode TE_{117}. The antenna structure consists of a rectangular DRA with three rectangular slots. One at the centre and other two inclined orthogonally with respect to centre slot. The bottom surface of substrate contains the modified feed structure in which two stubs of the same dimensions are connected orthogonally to main microstrip line to provide a phase difference of an odd multiple of $\lambda/2$ for circular polarization. DRA with excitation through modified aperture coupled feed structure provides the simulated and measured impedance bandwidths of 16.28% (22–25.9 GHz) and 15.06% (22.1–25.7) GHz. The antenna provides the simulated and measured gains of 8.4 dB and 7.9 dB. The antenna is deminiaturised by 61% by operating antenna at higher order mode. The designed antenna has potential for millimeter wave and 5G applications.

1. INTRODUCTION

Dielectric Resonator Antennas (DRAs) are a promising candidate to replace more traditional and conventional antennas especially at millimeter wave frequencies and beyond. This is mainly attributed to the fact that DRAs do not suffer from conduction losses and are characterized by high radiation efficiency when being excited properly. However, at millimeter wave frequencies, antenna dimensions are significantly reduced, which presents a challenge for ceramic based designs, due to the brittleness and difficulty of fabrication. The adoption of DRAs driven by higher order modes has the advantage of improving manufacturability at millimeter-wave frequencies. As a matter of fact, for a given resonant frequency fo, the size (volume) of a DRA operating on a higher order mode is much larger, typically by one order of magnitude or more, in comparison to that of the same DRA resonating at frequency fo on the relevant fundamental mode. Therefore, fabrication tolerances have a smaller relative impact on higher order modes. Millimeter wave communications at high frequencies suffer from high propagation losses due to absorption by oxygen molecules in the atmosphere. Hence, improving the gain is considered as one of the most important targets in antenna design for such frequencies. Also, in order to overcome multipath, improper line of sight between the transmitter and receiver and phase issues, due to rain or snow in the air, a circular polarized antenna is required to assure high quality transmission or reception. Very few circularly polarized antennas are available for the k-band. Antennas have been reported which employ an X-shaped slot excited by a rectangular substrate integrated waveguide and backed by circular cavity to cover the impedance and axial-ratio bandwidths 4.26% and 1.5%, respectively [17].

As per the literature survey, numerous techniques are enforced to scale back size of Microstrip antenna. Size may be reduced at a specific frequency by increasing the permittivity of substrate [1]. The

Received 12 September 2019, Accepted 19 November 2019, Scheduled 25 November 2019

* Corresponding author: Arti Vaish (vaisharti@gmail.com).

[1] Maharaja Surajmal Institute of Technology, India. [2] School of Engineering and Technology, Ansal University, Gurgaon, India.

reduction in antenna length by half may also be obtained by planning edge short patch [2, 3], shorting-pin-Loaded circular microstrip antenna [4]. An equilateral-triangular microstrip antenna [5] and a half-E-shaped patch antenna [6] design may also decrease the dimensions of an antenna. A quarter-size patch supported a shortening wall and having the probe at the edge to create an artificial magnetic wall has additionally been demonstrated [7]. Shapes like circular patch antenna [8] and slot-loaded meandered rectangular microstrip antenna [9] are additionally implemented. Structures like folded patch [10] is designed. These size reduction techniques degrade some antenna performance parameters. However, in contrast to microstrip antennas, size reduction techniques for the dielectric-resonator antenna are limited. For example, employing a shorted pin, meandered microstrip traces, or surface slots are common size-reduction techniques for microstrip antennas; however, they are not effective for reducing the dimensions of dielectric-resonator antennas. One common approach of reducing the dielectric-resonator antenna size is by using very high dielectric materials because dielectric-resonator antenna's size is inversely proportional to the dielectric constant at a fixed operational frequency. However, once the constant increases, the bandwidth decreases, and therefore, the radiation properties are degraded, because the radiation quality factor increases [11]. An antenna is designed, within which 10 split ring resonators (SRR) metamaterial structures are symmetrically etched on the radiation patch [18], and dielectric resonator antenna with metamaterial [19, 20] and FSS structure [22] are mentioned. MIMO antenna consists of four cylindrical DR antenna elements operational at 30 GHz with a bandwidth of one GHz is projected [21]. It has been shown very recently that even the elemental TE_{111} mode can give larger gain if the resonator's shape is modified [23]. The gain of the cylindrical HEM_{133} mode DRA is raised by introducing a very small air gap between the bottom plane and the resonator [24]. Novel DRA elements are projected quite recently in [25, 26].

In this paper a simple modified aperture coupled feeding line is used to achieve wider bandwidth. The percentage bandwidth is the ratio of the frequency range (highest frequency minus lowest frequency) divided by the center frequency. The DRA is excited at higher order mode TE_{117} which makes fabrication of the antenna easier at high frequency of 24 GHz. The other modes which are very close to the operating mode may be excited. These degenerate modes have different radiation patterns and may undesirably increase the cross-polarized field or even distort the radiation pattern of the antenna. Hence, the aspect ratio of DRA is carefully chosen such that only those higher order degenerate modes are generated, which have almost same radiation patterns and can be merged. The rectangular DRA comprises dimensions $(a * b * d)$, where a, b, d are length, width, and height of RDRA as demonstrated in Fig. 1(b). For this purpose, the DRA is tested for several aspect ratios (b/d) to operate on higher order mode TE_{117}, and then aspect ratio of 0.97 is finally selected for which modes TE_{155} and TE_{551} are generated along with TE_{117}.

2. RESONANT MODE CHARACTERISTICS

The modes mainly depend on the RDRA boundary and excitation conditions.

Electric walls of RDRA:

$$E_{\tan} = nXE = 0 \tag{1}$$

$$H_{nor} = n \cdot H = 0 \tag{2}$$

where E and H denote the electric and magnetic field intensities; n is the unit vector; $E_{\tan}$ is the tangential component of electric field; H_{nor} is the normal component of magnetic field.

Magnetic walls of RDRA:

$$H_{\tan} = nXH = 0 \tag{3}$$

$$E_{nor} = n \cdot E = 0 \tag{4}$$

The characteristic equation of RDRA is given as

$$\epsilon_r k_o^2 = k_x^2 + k_y^2 + k_z^2 \tag{5}$$

where $k_o \rightarrow$ Free space wave, $k_x, k_y, k_z \rightarrow$ Propagation constant in x, y, and z directions, $\epsilon_r \rightarrow$ Relative permittivity.

Transcendental equation for RDRA when fields are propagating in z-direction is

$$k_z \tan\left(\frac{k_z d}{2}\right) = \sqrt{(\epsilon_r - 1)\, k_o^2 - k_z^2} \tag{6}$$

The modal characteristics of antenna give rise to the field, i.e., resonant modes. These are known as eigen vectors and eigen values.

The resonant frequency can be given as follows:

$$(f_r)_{m,n,p} = \frac{c}{2\pi\sqrt{\mu\epsilon}}\sqrt{\left(\frac{m\pi}{a}\right)^2 + \left(\frac{n\pi}{b}\right)^2 + \left(\frac{p\pi}{d}\right)^2} \tag{7}$$

where m, n, p are the half-wave field variations along x, y, z directions.

a, b, d are length, width, and height of RDRA.

More number of modes along z-axis in RDRA can be generated either by increasing height d of RDRA or by increasing resonant frequency of RDRA.

3. ANTENNA CONFIGURATION

Figures 1(a), (b) show the geometry of the proposed antenna feed structure. The proposed antenna feed structure contains an epoxy ($\epsilon_s = 4.4$) substrate of dimensions $L_s * W_s$ and thickness 1.6 mm. There is a ground plane at the top of the substrate, which contains three rectangular slots. One at the centre, having dimensions $L_t * W_t$ and the other two inclined orthogonally with respect to central slot having dimensions $L_{t1} * W_{t1}$ and $L_{t2} * W_{t2}$, respectively. The bottom surface of the substrate contains a modified feed structure in which two stubs of the same dimensions $L_{b1} * W_{b1}$ and $L_{b2} * W_{b2}$ are connected orthogonally to main microstrip line of dimensions $L_m * W_m$. The design dimensions are summarized in Table 1. The modified microstrip line is designed such that two stubs and main microstrip feed provide a phase difference of an odd multiple of $\lambda/2$ in the signal along the three slots placed orthogonally over them. Hence, design of the modified feed line is based on the concept of phase change of input signal along the electrical length of the line. All the calculations are done using the formula:

$$\beta l = m\lambda/2 \quad \text{where } m = 1, 3, 5, 7 \ldots . \text{ (odd multiples)}$$

and βl refers to phase change of input signal along the electrical length.

Initially, the microstrip feed line width was set to have 50 ohm characteristic impedance along the line, but to obtain the appropriate results of the antenna, dimensions of the slots and microstrip feed line

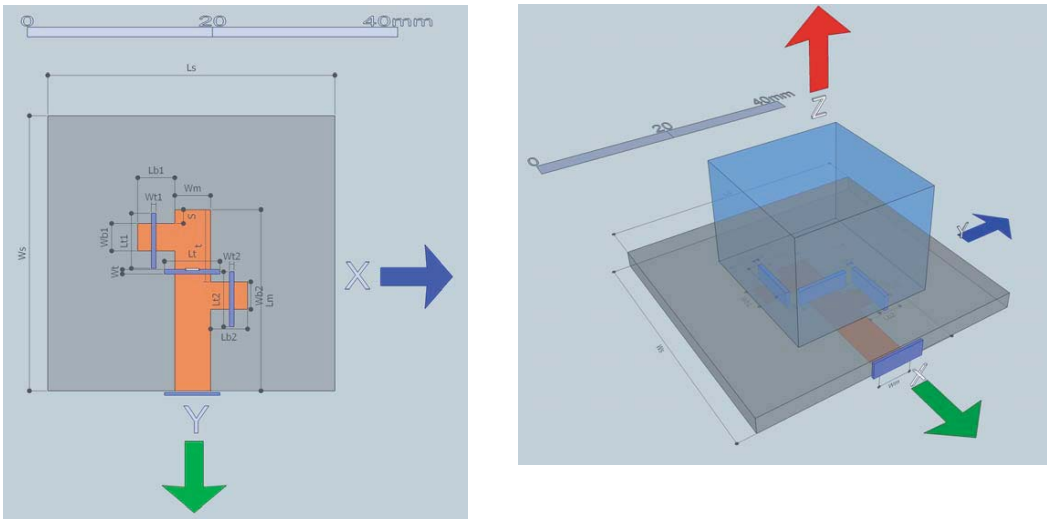

(a) (b)

Figure 1. (a) Design of modified aperture coupled feed. (b) Layout of designed RDRA.

Table 1. Dimensions of elements in antenna.

Elements	Dimensions	Elements	Dimensions
L_s	30 mm	L_{b1}	4 mm
W_s	30 mm	W_{b1}	2 mm
L_m	20 mm	L_{b2}	4 mm
W_m	2 mm	W_{b2}	2 mm
L_t	5 mm	s	1.25 mm
W_t	1 mm	t	7 mm
L_{t1}	5 mm	Substrate thickness	1.6 mm
W_{t1}	0.5 mm	Length of DRA	12 mm
L_{t2}	5 mm	Width of DRA	12 mm
W_{t2}	0.5 mm	Height of DRA	12.4 mm

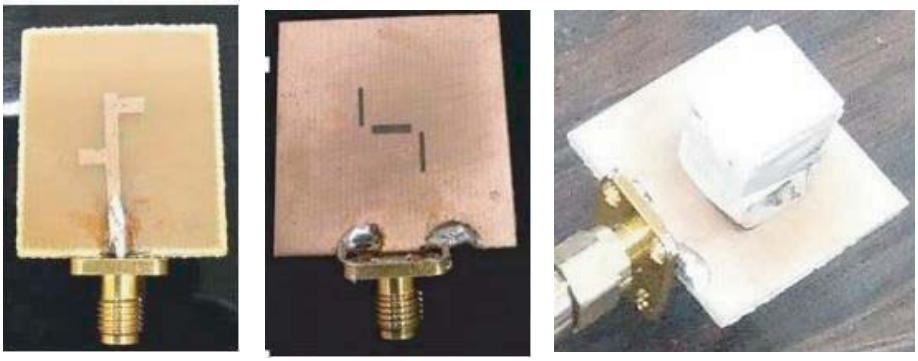

Figure 2. Fabricated prototype of the proposed antenna.

width are optimized using high-frequency structure simulator (HFSS) based on finite element method (FEM). Fig. 2 shows the fabricated prototype of the proposed feed and antenna structure.

4. OPERATING PRINCIPLE

Using dielectric waveguide model, resonance frequencies of the first few higher order modes are calculated [3] for different ratios of b/d with $a = b$, where a, b, d are length, width, and height of RDRA as demonstrated in Fig. 1(b).

Aspect ratio is chosen between 0.4 and 0.75 for single mode operation (TE_{11p}), for $p = 5, 7, 9, 11$, where p represents modes in z direction. In Fig. 3, various TE_{11p} modes are plotted against their aspect ratio using the transcendental equation. In a rectangular cavity, modes are designated as TE_{mnp}, where m, n, p are the number of half wave variations in x, y, z directions, respectively. The ratio b/d and $K_o d$ are plotted on the x-axis and y-axis of Fig. 3. As can be observed from Fig. 3, the resonant frequencies of these modes decrease with an increase of ratio b/d. Transcendental Equation (6) of rectangular DRA provides a complete solution of propagation constants, i.e., kx, ky, and kz. The propagation constant gives rise to resonant frequency with the help of characteristic Equation (5). The wave numbers kx, ky, and kz are in x, y, and z directions, respectively. The free space wave number is K_o. The exact solution of RDRA resonant frequency can be determined from combined solution of transcendental equation and characteristic equation. It is demonstrated in Fig. 3 that the mode distribution of a rectangular DRA is affected by its aspect ratios. When dimensions of the DRA are chosen improperly, other modes that are very close to the operating mode may be excited. In general, these degenerate modes have different

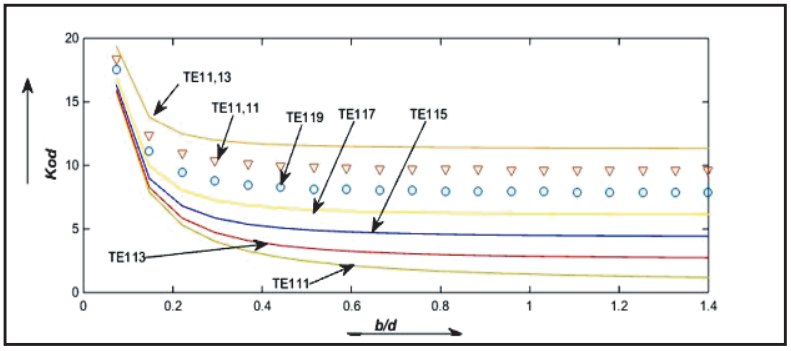

Figure 3. Various mode curves as a function of b/d: (for $\epsilon = 10$, $a = b$).

radiation patterns and may undesirably increase the cross-polarized field or even distort the radiation pattern of the antenna.

The aspect ratio and the dimensions for the concerned modes are summarized in Table 2.

Table 2. Modes, aspect ratio and dimensions.

Mode generated	Aspect ratio	a (mm)	b (mm)	d (mm)
TE^{y}_{113}	0.55	2.7	2.7	4.9
TE^{y}_{115}	0.65	4	4	6.1
TE^{y}_{117}	0.54	2.6	2.6	8.9
TE^{y}_{119}	0.28	3	3	10.7

As can be observed from Table 2, for a given resonant frequency fo the size (volume) of a DRA operating on a higher order mode is much larger, typically by one order of magnitude or more, in comparison to that of the same DRA resonating at frequency fo on the relevant fundamental mode. This technique provides deminiaturisation and makes fabrication of DRA easier at high frequency.

Figure 4 shows the radiation pattern of simulated antenna at 24 GHz. Excitation of other neighboring modes is depicted in this figure. These modes are merged, when being excited through modified feed. Choosing appropriate b/d ratio as 0.97, only those modes are generated which have radiation pattern the same as that of dominant mode TE^{y}_{117}.

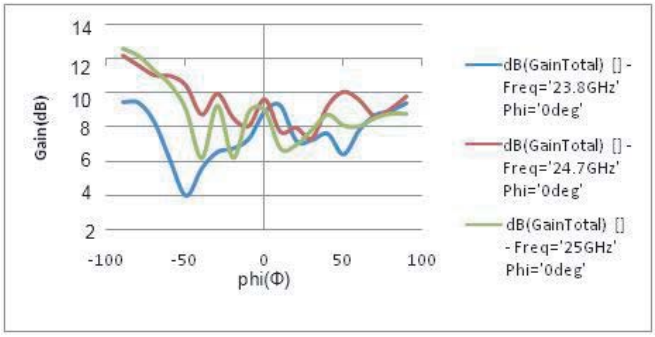

Figure 4. Radiation pattern of three modes excited simultaneously.

Figure 5 depicts the modal distribution of generated modes TE_{113}, TE_{115}, TE_{117}, representing number of half wave variations in z direction. The modes are spectral resolution of electromagnetic

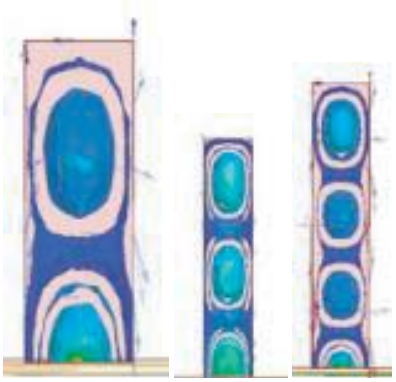

Figure 5. Mode distribution TE_{113}, TE_{115}, TE_{117}.

Figure 6. Return loss showing simultaneous excitation of the three modes.

fields of waves radiated by the RDRA. Radiating behavior of the antenna can be predicted by modes. The dominant mode corresponds to the lowest resonant frequency. The modes are generated based on the current distribution on the surface of antenna due to field perturbations. Resonant modes are field structures that can exist inside the DRA. Modes are the pattern of motion which repeat itself sinusoidally. Different modes exist at different resonating frequencies. They can be merged, separated, and mixed depending upon the requirements. When shaping the dielectric resonator, different modes can be excited, which results in a wide bandwidth. The reflection coefficient is also known as S_{11} or return loss. The impedance bandwidth of the antenna is defined as the range of frequencies over which the return loss is < 10 dB. The reflection coefficient characteristics as the function of frequency of antenna is plotted in Fig. 6. It is demonstrated in Fig. 6 that the antenna exhibits < 10 dB reflection coefficient over frequency band at (22–26 GHz). Simultaneous generation and merging of three modes is also depicted.

5. RESULTS AND DISCUSSION

The designed antenna is simulated in software HFSS, so the prototype of antenna has been designed in lab. The varied simulated and experimental results are mentioned in this section. The simulated and measured frequency responses of S_{11} parameter of the projected antenna excited by modified aperture coupled feed structure is shown in Fig. 6, Fig. 7, and Fig. 8. DRA with excitation through modified aperture coupled feed structure provides simulated and measured impedance bandwidths of 16.28% (22–25.9 GHz) and 15.06% (22.1–25.7 GHz).

The antenna provides simulated and measured gains of 8.4 dB and 7.9 dB as shown in Fig. 9. All the results are summarized in Table 3.

The left hand circular polarization (LHCP) and right hand circular polarization (RHCP) radiation

Figure 7. Measurement setup.

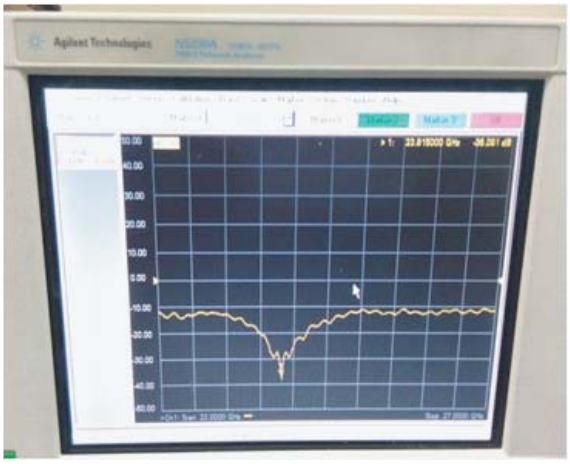

Figure 8. Measured S_{11}.

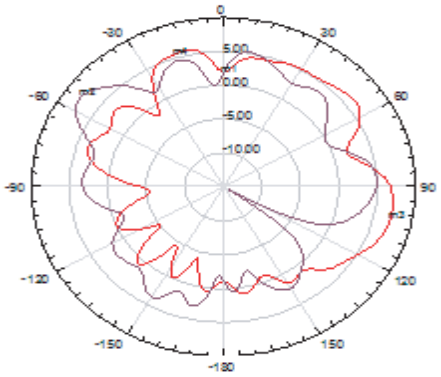

(a)

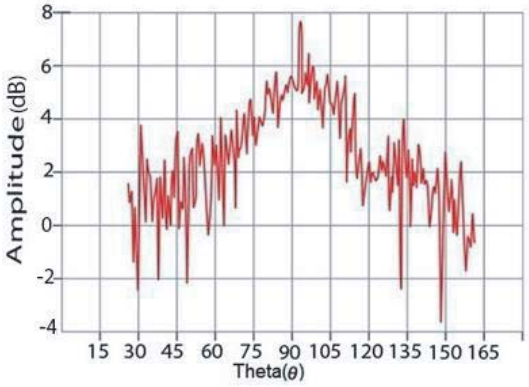

(b)

Figure 9. Simulated and measured gain of antenna.

Table 3. Performance table of designed antenna.

Parameter	Simulated	Measured
Impedance BW	16.28% (22–25.9 GHz)	15.06% (22.1–25.7 GHz)
Gain	8.4 dB	7.9 dB

Table 4. Comparison with other antennas designs.

Ref.	fr (GHz)	Type of Antenna	BW_{Im} (%)	BW_{AR} (%)	Antenna size
[12]	30	CDRA	3.33	NA	3.2×3.1
[13]	25.8	CDRA	2.15		5.03×9.08
[14]	24	RDRA	2.08	NA	$1.5 \times 1.5 \times 3.02$
[15]	27.5	CDRA	54.5	NA	2.5×2
[16]	28	Fabry parot DRA	14.28	NA	$5.35 \times 5.35 \times 0.8$
This antenna	24	RDRA	15.06	5.88	$12 \times 12 \times 12.4$

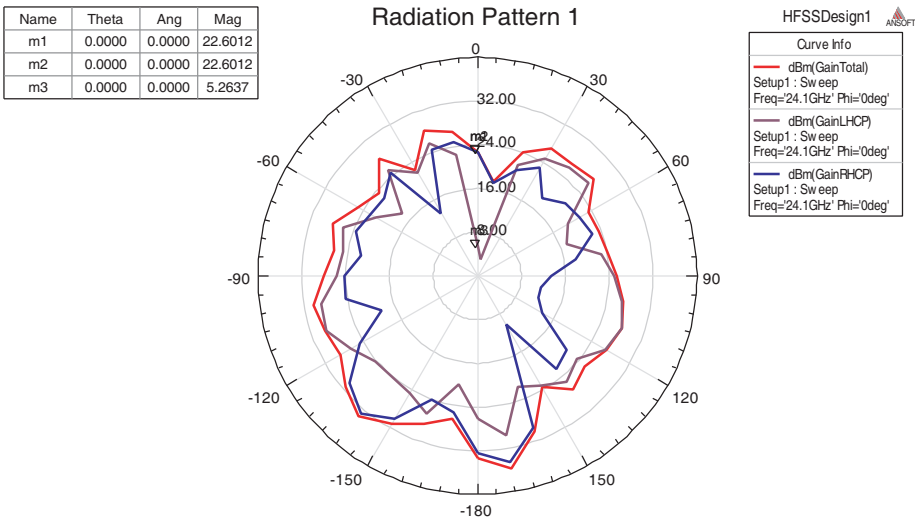

Figure 10. *E* plane radiation pattern.

patterns in direction (phi = 0°) for the frequency 24.1 GHz is shown in Fig. 10. It is observed that the RHCP is stronger than the LHCP in the direction (phi = 0°) by 17 dB at 24.1 GHz which confirms that the antenna provides RHCP radiations. Furthermore, polarization is reversed from RHCP to LHCP if the stub in the microstrip line and the orthogonal slot placement is mirror reversed. In Table 4, some of the performance parameters of the proposed antenna are compared with existing antennas.

6. CONCLUSION

A Rectangular Dielectric Resonator Antenna (RDRA) with a modified feeding line is designed and investigated at 24 GHz. The antenna deminiaturization is achieved by operating the antenna at higher order mode. The technique of mode control, by varying aspect ratio, has been investigated. The modified feed line, used for exciting RDRA, contributes to a wide bandwidth operation and circular polarization. The antenna can be used for robust and high quality signal reception. DRA with excitation through modified aperture coupled feed structure provides simulated and measured impedance bandwidths of 16.28% (22–25.9 GHz) and 15.06% (22.1–25.7) GHz. The antenna provides simulated and measured gains of 8.4 dB and 7.9 dB. The antenna is deminiaturised by 61% by operating the antenna at higher order mode. Thus, it has potential for millimeter wave, radar, and 5G applications.

REFERENCES

1. Wong, K.-L., *Compact and Broadband Microstrip Antennas*, Vol. 168, John Wiley & Sons, 2004.
2. Liu, Z. D., P. S. Hall, and D. Wake, "Dual-frequency planar inverted-F antenna," *IEEE Transactions on Antennas and Propagation*, Vol. 45, No. 10, 1451–1458, 1997.
3. Yaduvanshi, R. S. and H. Parthasarathy, *Rectangular Dielectric Resonator Antennas*, Springer, New Delhi, India, 2016.
4. Waterhouse, R., "Small microstrip patch antenna," *Electronics Letters*, Vol. 31, No. 8, 604–605, 1995.
5. Wong, K.-L. and S.-C. Pan, "Compact triangular microstrip antenna," *Electronics Letters*, Vol. 33, No. 6, 433–434, 1997.
6. Chair, R., C.-L. Mak, K.-F. Lee, K.-M. Luk, and A. A. Kishk, "Miniature wide-band half U-slot and half E-shaped patch antennas," *IEEE Transactions on Antennas and Propagation*, Vol. 53, No. 8, 2645–2652, 2005.

7. Kishk, A. A., K. F. Lee, W. C. Mok, and K.-M. Luk, "A wide-band small size microstrip antenna proximately coupled to a hook shape probe," *IEEE Transactions on Antennas and Propagation*, Vol. 52, No. 1, 59–65, 2004.
8. Wong, K.-L., C.-L. Tang, and H.-T. Chen, "A compact meandered circular microstrip antenna with a shorting pin," *Microwave and Optical Technology Letters*, Vol. 15, No. 3, 147–149, 1997.
9. Lu, J. H. and K. L. Wong, "Slot-loaded meandered rectangular microstrip antenna with compact dual-frequency operation," *Electronics Letters*, Vol. 34, No. 11, 1048–1049, 1998.
10. Chair, R., K. M. Luk, and K. F. Lee, "Small dual patch antenna," *Electronics Letters*, Vol. 35, No. 10, 762–764, 1999.
11. Mongia, R. K. and A. Ittipiboon, "Theoretical and experimental investigations on rectangular dielectric resonator antennas," *IEEE Transactions on Antennas and Propagation*, Vol. 45, No. 9, 1348–1356, 1997.
12. Sharawi, M. S., S. K. Podilchak, M. T. Hussain, and Y. M. M. Antar, "Dielectric resonator based MIMO antenna system enabling millimetre-wave mobile devices," *IET Microwaves, Antennas & Propagation*, Vol. 11, No. 2, 287–293, 2017.
13. Mrnka, M., M. Cupal, Z. Raida, A. Pietrikova, and D. Kocur, "Millimetre-wave dielectric resonator antenna array based on directive LTCC elements," *IET Microwaves, Antennas & Propagation*, Vol. 12, No. 5, 662–667, 2018.
14. Haddad, A., M. Aoutoul, K. Rais, and M. Essaaidi, "Rectangular dielectric resonator antenna (RDRA) for anti-collision short range radar (SRR) application," *2016 International Conference on Electrical and Information Technologies (ICEIT)*, 237–239, IEEE, 2016.
15. Parchin, N. O., M. Shen, and G. F. Pedersen, "Mm-wave dielectric resonator antenna (DRA) with wide bandwidth for the future wireless networks," *International Conference on Microwave, Radar and Wireless Communications (MIKON)*, 1–4, 2016.
16. Parchin, N. O., M. Shen, and G. F. Pedersen. "Wideband Fabry-Pérot resonator for 28 GHz applications," *2016 IEEE International Conference on Ubiquitous Wireless Broadband (ICUWB)*, 1–4, IEEE, 2016.
17. Elboushi, A., O. M. Haraz, and A. Sebak, "Circularly-polarized SIW slot antenna for MMW applications," *2013 IEEE Antennas and Propagation Society International Symposium (APSURSI)*, 648–649, IEEE, 2013.
18. Li, R., Q. Zhang, Y. Kuang, X. Chen, Z. Xiao, and J. Zhang, "Design of a miniaturized antenna based on split ring resonators for 5G wireless communications," *2019 Cross Strait Quad-Regional Radio Science and Wireless Technology Conference (CSQRWC)*, 1–4, IEEE, 2019.
19. Gharsallah, H., L. Osman, and L. Latrach, "Circularly polarized two-layer conical DRA based on metamaterial," *Microwave and Optical Technology Letters*, Vol. 59, No. 8, 1913–1919, 2017.
20. Zhu, C., T. Li, K. Li, Z.-J. Su, X. Wang, H.-Q. Zhai, L. Li, and C.-H. Liang, "Electrically small metamaterial-inspired tri-band antenna with meta-mode," *IEEE Antennas and Wireless Propagation Letters*, Vol. 14, 1738–1741, 2015.
21. Sharawi, M. S., S. K. Podilchak, M. T. Hussain, and Y. M. M. Antar, "Dielectric resonator based MIMO antenna system enabling millimetre-wave mobile devices," *IET Microwaves, Antennas & Propagation*, Vol. 11, No. 2, 287–293, 2017.
22. Akbari, M., S. Gupta, M. Farahani, A. R. Sebak, and T. A. Denidni, "Gain enhancement of circularly polarized dielectric resonator antenna based on FSS superstrate for MMW applications," *IEEE Transactions on Antennas and Propagation*, Vol. 64, No. 12, 5542–5546, 2016.
23. Fakhte, S., H. Oraizi, and L. Matekovits, "Gain improvement of rectangular dielectric resonator antenna by engraving grooves on its side walls," *IEEE Antennas and Wireless Propagation Letters*, Vol. 16, 2167–2170, 2017.
24. Mrnka, M. and Z. Raida, "Gain improvement of higher order mode dielectric resonator antenna by thin air gap," *2016 International Conference on Broadband Communications for Next Generation Networks and Multimedia Applications (CoBCom)*, 1–3, IEEE, 2016.

25. Mrnka, M. and Z. Raida, "Enhanced-gain dielectric resonator antenna based on the combination of higher-order modes," *IEEE Antennas and Wireless Propagation Letters*, Vol. 15, 710–713, 2015.
26. Mrnka, M. and Z. Raida, "Linearly polarized high gain rectangular dielectric resonator antenna," *2016 10th European Conference on Antennas and Propagation (EuCAP)*, 1–4, IEEE, 2016.